Physica Medica 67 (2019) 9–19

Contents lists available at ScienceDirect

Physica Medica

journal homepage: www.elsevier.com/locate/ejmp

Original paper

The essential role of radiobiological figures of merit for the assessment and comparison of beam performances in boron neutron capture therapy

L. Provenzano[a,b], H. Koivunoro[c], I. Postuma[d], J.M. Longhino[a], E.F. Boggio[a], R.O. Farías[e], S. Bortolussi[d,f], S.J. González[a,b,*]

[a] Comisión Nacional de Energía Atómica (CNEA), Av. Gral Paz 1499 (1650), San Martín, Buenos Aires, Argentina
[b] Consejo Nacional de Investigaciones Científicas y Técnicas (CONICET), Godoy Cruz 2290 (1425), C.A.B.A., Argentina
[c] Neutron Therapeutics, 1 Industrial Drive, Danvers, MA 01923, United States
[d] Istituto Nazionale di Fisica Nucleare (INFN), Unit of Pavia, Via Bassi 6, 27100 Pavia, Italy
[e] Universidad Favaloro, FICEN, Av. Belgrano 1723 (1093), C.A.B.A., Argentina
[f] Department of Physics, University of Pavia, Via Bassi 6, 27100 Pavia, Italy

ARTICLE INFO

Keywords:
BNCT
UTCP
TCP
Neutron beam performance

ABSTRACT

Purpose: Boron Neutron Capture Therapy (BNCT) is a treatment modality that uses an external neutron beam to selectively inactive boron10-loaded tumor cells. This work presents the development and innovative use of radiobiological probability models to adequately evaluate and compare the therapeutic potential and versatility of beams presenting different neutron energy spectra.

M&M: Aforementioned characteristics, collectively refer to as the performance of a beam, were defined on the basis of radiobiological probability models for the first time in BNCT. A model of uncomplicated tumor control probability (*UTCP*) for HN cancer was introduced. This model considers a *NTCP* able to predict severe mucositis and a *TCP* for non-uniform doses derived herein. A systematic study comprising a simplified HN cancer model is presented as a practical application of the introduced radiobiological figures of merit (FOM) for assessing and comparing the performance of different clinical beams. Applications involving treated HN cancer patients were also analyzed.

Results: The maximum *UTCP* proved suitable and sensitive to assess the performance of a beam, revealing particularities of the studied sources that the physical FOMs do not highlight. The radiobiological FOMs evaluated in patients showed to be useful tools both for retrospective analysis of the BNCT treatments, and for prospective studies of beam optimization and feasibility.

Conclusions: The presented developments and applications demonstrated that it is possible to assess and compare performances of completely different beams fairly and adequately by assessing the radiobiological FOM *UTCP*. Thus, this figure would be a practical and essential aid to guide treatment decisions.

1. Introduction

Boron Neutron Capture Therapy (BNCT) is an advanced form of particle radiotherapy that requires the intravenous administration of a tumor-selective boron-10 compound. After an adequate time for the compound to accumulate in tumor, the target region is irradiated with a suitable neutron beam, producing highly localized dose of alpha and lithium particles released after thermal neutron capture [1].

Considerable efforts are being devoted to the design of neutron beams with the adequate physical characteristics to deliver a therapeutic dose to the tumor, exploiting the selectivity of boron bio-distribution. Modifications or new designs of beam shaping assemblies, aimed at moderating and collimating neutron beams for clinical application, are being proposed for accelerators and for reactor-based centers. It is thus important to establish criteria to evaluate the clinical performance of these beams, using as a reference the outcomes obtained in facilities that have already treated patients, for which it is possible to draw conclusion on BNCT safety and effectiveness.

The development of more refined criteria to understand the potentiality of a neutron beam is ongoing. Traditionally, in-air free-beam physical characteristics have been almost the only common base on which clinical beams were and continue to be designed, optimized and compared with each other. For example, the technical report on neutron capture therapy published by IAEA in 2001 [2] indicates that the

* Corresponding author at: Comisión Nacional de Energía Atómica (CNEA), & CONICET Argentina, Av. Gral. Paz 1499, (1650) San Martín, Buenos Aires, Argentina.
E-mail address: srgonzal@cnea.gov.ar (S.J. González).

https://doi.org/10.1016/j.ejmp.2019.09.235
Received 20 June 2019; Received in revised form 9 September 2019; Accepted 14 September 2019
Available online 11 October 2019

two main characteristics of interest for a clinical beam are intensity, and quality. The first determines the treatment time, while the latter relates to the type, the energy and relative intensity of each radiation components present in the incident beam. These figures of merit proved suitable to guarantee adequate and safe epithermal beams for the treatment of deep-seated tumors. However, their usefulness to assess the therapeutic potential and the versatility of a beam for a given treatment is limited. Moreover, beams with very different energy spectra cannot be fairly compared. A pioneering work of different beam and treatment strategies comparisons incorporating other types of figures, such as a probability of tumor control (*TCP*), was published by Wheeler et al. in 1999 [3]. These authors showed how, from a simple *TCP* model developed for brain tumors, it was possible to assess the quality of various beams in a relative sense by setting a maximum tolerable photon equivalent dose in normal tissue. Although the analysis contemplated epithermal beams, simplified models and single-field irradiations only, this work marked a very important starting point and opened new horizons to understand and compare the therapeutic potential of different BNCT beams.

Since that time, new research in BNCT has emerged offering not only more accurate models of photon iso-effective dose calculation, but also suitable probability models that describe the dose-effect relationship observed in the treatment of humans for both tumor and normal tissue. In this work, the use of radiobiological figures of merit (FOMs) specially developed for BNCT were proposed

1. to assess the therapeutic potential and versatility of a beam, that collectively are referred to as “the performance of a beam”, and
2. to compare the performance of existing or developing beams regardless of their spectral characteristics.

The starting point of this work is based on the probability models published in González et al. (2012) [4] for treatment of head and neck cancer. The first step is the development of the *TCP* model for non-uniform dose distributions. From this model and the normal tissue complication probability (*NTCP*) introduced in González et al. (2017) [5], the Uncomplicated Tumor Control Probability (*UTCP*) is defined and proposed.

The existing neutron sources at the Argentine RA-6 Reactor (RA-6 B2) and at the Finnish Research Reactor (FiR 1) used in the clinic of BNCT for the treatment of both superficial and deep-seated tumors were evaluated and compared. In addition, the performance of two realistic epithermal beam designs, that include modifications of the current mixed thermal-epithermal beam of the RA-6 reactor and the proton Radiofrequency Quadrupole accelerator (RFQ) manufactured by INFN in Italy [6], were also assessed and discussed. A systematic study comprising a standard geometry for HN cancer is presented as a practical application of the introduced radiobiological figures of merit for assessing and comparing the performance of the different BNCT beams.

Finally, the application of the introduced figures in a real clinical context involving HN cancer patients treated in Finland is analyzed and the results are discussed in the light of physical characteristics of the studied beams and treatment outcomes.

2. Materials and methods

2.1. Current status of desired neutron beam parameters based on IAEA recommendation

In 2001, a technical document with the status of neutron capture therapy was published by IAEA [2]. The report compiles an extensive analysis of the scientific and technological development achieved up to the publication date. At that time, the international interest about reactor-based BNCT was mainly focused in clinical trials of brain tumors. Since for target volumes well below the surface epithermal beams are preferred (with the epithermal energy range defined between 0.5 eV and 10 keV), a set of desired parameters for these intermediate energy beams was recommended to guarantee an adequate and safe treatment.

According to the IAEA report, intensity and quality are the two main characteristics of interest to describe a neutron beam. What follows summarizes the figures of merit suggested for epithermal beams and the recommended values. Although it was not clearly stated in the report, it is expected that all parameters correspond to the average values over the beam aperture at the exit port (i.e., at the patient position). Recommended figures of merit are also summarized on Table 3.

1. *Epithermal beam intensity*: based on clinically relevant data about tumor boron concentration values and reasonable treatment times (~1 h), the recommended minimum value is 10^9 epithermal neutrons $cm^{-2}\,s^{-1}$.
2. Four parameters under free beam conditions were suggested to describe the incident beam quality:
   a. *The fast neutron component*: fast neutrons (> 10 keV) in the incident beam produce undesired intermediate-LET protons that are more biologically damaging than photons and are not selective for tumor. The dose from this component should be reduced as much as possible while epithermal neutrons are maximized. The recommended maximum value is 2×10^{-13} Gy cm^2 per epithermal neutron
   b. *The gamma ray component*: gamma radiation in the incident beam is also an undesired radiation due to its non-selective dose deposition. The recommended maximum value is 2×10^{-13} Gy cm^2 per epithermal neutron.
   c. *The ratio between the thermal flux and the epithermal flux*: thermal neutrons in the incident beam are expected to increase the dose near the surface. To lower the probability of radiotoxic effects in superficial healthy tissues, the recommended maximum ratio of the thermal flux to epithermal flux is 0.05.
   d. *The ratio between the total neutron current and the total neutron flux*: this figure of merit provides a measure of the fraction of neutrons in the forward direction. The higher the value, the lower the unwanted doses to other tissues and the greater the flexibility in patient positioning along the beam. The minimum target value recommended is 0.7.

Low to intermediate energy neutron beams have been used in the clinic of BNCT to treat different tumor targets [7,8]. However, IAEA recommendations to establish the characteristics desired for NCT were only addressed for epithermal beams. The lack of suitable figures for low energy neutron beams designed to treat superficial tumors prompted the introduction of a similar set of FOMs in this work. This is shown and discussed in Section 2.4. Moreover, to establish objective criteria based on tridimensional dose distributions that allow an adequate comparison of the therapeutic potential of the neutron beams regardless of their energy spectra, radiobiological figures of merit were introduced and discussed.

2.2. Model for dose calculation

The dose in BNCT is due to a mixed field of radiation, made up of high LET alpha particles and lithium ions coming from thermal neutron capture in ^{10}B, intermediate LET protons produced as a result of the thermal neutron capture reaction by ^{14}N and neutron elastic collision with ^{1}H nuclei, and low LET gamma-ray present in the neutron beam and arising from thermal neutron capture in ^{1}H. Traditionally, photon-equivalent dose has been calculated in BNCT weighting each component with fixed (dose and dose rate independent) Relative Biological Effectiveness (RBE) and Compound Biological Effectiveness (CBE) factors [9]. The dose obtained with this model is commonly referred to as “RBE-weighted dose” and expressed in Gy-Eq.

As the standard RBE/CBE dosimetry model was proven to fail in explaining the BNCT outcome when compared to conventional photon

radiotherapy [4], a more accurate model was employed in this work. The photon iso-effective dose formalism translates BNCT doses into photon doses with the same biological effect, without using RBE or CBE factors [4]. Essentially, it defines the photon iso-effective dose as the photon reference dose that produces the same effect (i.e. tumor control or normal tissue toxicity) as a given combination of the absorbed dose components of BNCT [5]. Since predictions based on this model were shown to be compatible with the observed clinical outcome for different BNCT protocols (e.g., in the Argentine [10,11] and Finnish BNCT treatments of cutaneous melanoma and recurrent head and neck cancer [8]), photon iso-effective doses were estimated in the present work. The unit Gy(IsoE) is used for this model.

2.3. Radiobiological and clinical perspective for neutron beam assessment

The aim of radiotherapy is to achieve a high probability of local tumor control at a low risk of normal tissue complications. In order to estimate the expected success of a radiation treatment, suitable models for computing the tumor control probability (*TCP*) and the normal tissue complication probability (*NTCP*) are required. Probability models are mathematical expressions that describe the probability of a given effect. The more general and sophisticated the model is, the more complex the expression results. However, recognizing which particularities of the radiation treatment must be represented in full detail to predict the effects, probability models are very valuable tools. Among the most salient features, they manage to condense tridimensional information into a single score. In BNCT, these models can be used to predict the probability of success of a radiation treatment, or as clinically relevant figures of merit to assess the therapeutic potential of a beam. Moreover, different beams can be inter-compared on these bases, regardless their energy spectra and physical characteristics.

The development of suitable probability models for BNCT is growing in recent years due to the introduction of more adequate dose calculation models that explain the clinically observed effects in light of the results obtained with conventional photon radiotherapy [4,5,12,13]. Examples of the probability models can be found in Laramore et al. (1997) [14], González et al. [4,5] and Farías et al. [15].

The following shows the extension of the existing *TCP* models for HN cancer to take into account inhomogeneous tumor dose distributions. In addition, the uncomplicated tumor control probability (*UTCP*) is defined from the derived *TCP* model for BNCT, and the dose-limiting normal tissue complication probability for HN cancer presented in González et al. [5].

2.3.1. Tumor control probability for inhomogeneous dose distributions

It is widely known that in radiation therapy, the release of a homogeneous high dose to the tumor region is one of the cornerstones [16]. Since, under this condition, the average absorbed dose is representative of the dose to the target volume, most *TCP* models do not need to deal with large dose inhomogeneity. In BNCT, the dose distribution varies significantly with depth, and despite tailored treatment planning using multiple portals, dose uniformity conditions are virtually impossible to achieve, particularly in large tumor volumes.

In González et al. [5] tumor control probability models for photons (TCP_R) and for the mixed field BNCT radiation (*TCP*) were introduced. The proposed expressions are valid for uniform doses, and take into account fir first-order repair of sublethal damage and synergistic interactions between the main different radiations in BNCT. The parameters of the *TCP* models were determined using dose-response curves obtained from photon and BNCT studies performed in the hamster cheek pouch *in-vivo* models of oral cancer [5]. Since this animal model has been extensively used as a surrogate model for human oral cancers [17–20], the proposed expressions with the obtained parameters were considered radiobiological figures of merit potentially useful to assess and compare head and neck treatments with photons and BNCT.

Target volumes of HN cancer patients treated with BNCT are typically large, ranging from 20 cm^3 to 400 cm^3 [21,8,22]. Therefore, differences over 20% between maximum and minimum values of the tumor dose distribution are expected. The equivalent sub-volume model introduced by González and Carando [23] was applied to the uniform dose *TCP* models for photons and for BNCT mentioned above, in order to handle the inhomogeneous dose distributions. The irradiation using photons is a particular case of the more general scenario combining different radiation qualities, thus it is enough to develop the *TCP* model for inhomogeneous doses for BNCT. The mathematical derivation of the model is presented in Section 3.1 along with examples that highlight the importance of considering the inhomogeneous tumor dose distributions in the *TCP* calculation.

2.3.2. Uncomplicated tumor control probability

The tumor control and normal tissue complication probabilities can be combined to determine both the positive and detrimental effects of a given treatment into a single parameter. In its simplest form, the treatment utility is given as the uncomplicated tumor control probability (*UTCP*), defined as the probability for controlling a given tumor without complications in single nearby healthy organ or tissue. Assuming that tumor control and normal tissue complications are statistically independent processes, the *UTCP* is given by

$$UTCP = TCP(1 - NTCP). \quad (1)$$

By definition, the *UTCP* takes values between 0 and 1. Thus, the closer the value of the *UTCP* to 1, the higher the probability of uncomplicated tumor control. Given a number of patients with (ideally) equal clinical scenarios, the *UTCP* can be interpreted as the fraction of those patients that is expected to be cured without complications. Fig. 1 shows a schematic example of the *UTCP* as a function of the irradiation time. From the *UTCP* curve, it is possible to calculate the optimal treatment time t_{opt} for which the probability of controlling the tumor without complication is maximized.

Expression (1) is now introduced for the case of HN cancer treatments with BNCT using the *TCP* model derived for inhomogeneous dose distributions in this work (see Section 3.1) and the *NTCP* model introduced in González et al. [5].

NTCP models that can predict mucositis grade 3 or higher (≥G3) after head and neck cancer radiotherapy with photons and with BNCT were introduced in González et al. [5]. The proposed model for a single-fraction photon reference dose D_R is given by

$$NTCP(D_R) = \frac{1}{\sqrt{2\pi}} \int_{-\infty}^{s'} exp\left(-\frac{t^2}{2}\right) dt,$$

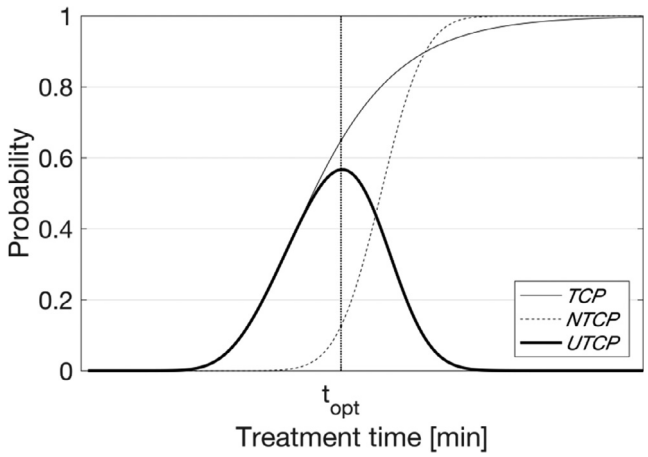

Fig. 1. Uncomplicated tumor control probability (UTCP) as a function of treatment time, for a single tumor with probability TCP to be controlled, and a single dose-limiting normal tissue with probability NTCP of unacceptable complications.

where

$$s' = \frac{D_R\left(1 + \frac{D_R G_R(\theta)}{(\alpha/\beta)_R}\right)/\left(1 + \frac{2G_R(\theta)}{(\alpha/\beta)_R}\right) - TD_{50}}{m \bullet TD_{50}} \quad (2)$$

In Eq. (2), $(\alpha/\beta)_R$ is the ratio of the coefficients of the single fraction LQ model and m and TD_{50} are the slope of the *NTCP* vs. dose curve and the tolerance dose for a complication probability of 0.5, respectively. In particular, values of $(\alpha/\beta)_R$, m and TD_{50} equal to 10 Gy, 0.17 and 39.8 Gy, respectively, were taken or calculated from Strigari et al. [24]. The time factor G_R was computed for fast and slow characteristic repair times $t_{0f} = 27/ln2$ min and $t_{0s} = 150/ln2$ min [25].

Let $D_1, \cdots, D_4$ denote the boron, thermal neutron, fast neutron and gamma uniform absorbed dose components of the mixed field BNCT radiation. The complication probability after a BNCT irradiation $NTCP = NTCP(D_1, \cdots, D_4)$ is obtained by replacing D_R in expression (2) by$D_R = D_R(D_1, \cdots, D_4)$

$$D_R(D_1, \cdots, D_4) = \frac{1}{2}\frac{(\alpha/\beta)_R}{G_R}\left(\sqrt{1 + \frac{4G_R}{\alpha_R(\alpha/\beta)_R}\left(\sum_{i=1}^{4}\alpha_i D_i + \sum_{i=1}^{4}\sum_{j=1}^{4} G_{ij}(\theta)\sqrt{\beta_i\beta_j}D_i D_j\right)} - 1\right) \quad (3)$$

Table 1 lists the radiobiological parameters of the *NTCP* model for the reference radiation and for BNCT used for calculation in this work. It is worth mentioning that in González et al. [5] this *NTCP* model proved suitable to predict the toxicity outcome of small cohort of patients treated within the HN cancer clinical trial carried out in Finland with BNCT. Afterwards, the predictive power of the model was assessed using the whole cohort of 30 patients reinforcing the previous results: the predicted number of patients that should develop mucositis ≥ G3 coincides with the observed outcome. Details of this work are beyond the scope of this paper and will be published elsewhere.

2.4. Studied neutron beams

Four neutron sources have been considered in this work. These sources were represented in the dosimetry calculations by angular-flux probability density functions or by a track-by-track description at a plane near the exit port. The first two correspond to the existing, well-characterized, clinical beams operated by the National Atomic Energy Commission of Argentina (CNEA) at the RA-6 Reactor (named, RA-6 B2) and by the Technical Research Centre of Finland (VTT) at the Finnish Reactor (named, FiR 1) [26,27]. In addition, two realistic epithermal beam designs, based on suitable modifications of the B2 clinical beam and on the proton Radiofrequency Quadrupole accelerator manufactured by INFN, were also studied. Following, the general characteristics of these beams are described. The corresponding neutron-energy spectra and depth-flux profiles in the standard water phantom are shown in Fig. 2. All the calculations were performed with MCNP Monte Carlo code [28]. Results shown have statistical uncertainties of less than 1%.

Table 1
Radiobiological parameters of the *NTCP* model (± 1SD) for the reference radiation and for BNCT based on in vivo oral cancer model data (González et al., 2017).

	NTCP $m = 0.17$, $TD_{50} = 39.8$ Gy	
	Alpha (Gy^{-1})	Beta (Gy^{-2})
^{60}Co or 6MV LINAC		
Reference radiation	0.35	0.035
FCCT (RA-3 reactor)		
Beam gamma photons	0.35	0.035
Neutrons	2.47 ± 0.03	~0
Boron (L-BPA-F)	3.09 ± 0.03	~0

FCCT: Thermal column central facility of the RA-3 nuclear reactor (Buenos Aires, Argentina); L-BPA-F: L-boronophenylalanine fructose.

2.4.1. RA-6 clinical beam B2

The BNCT clinical facility located at Bariloche Atomic Center (CNEA, Argentina) was developed in RA-6 open-pool reactor and it currently operates with 20% enriched U-235 fuel elements at a nominal power of 1 MW. This facility provides the so-called clinical beam RA-6 B2 with a mixed thermal-epithermal neutron spectral composition especially tuned for treating shallow tumors (Fig. 2A). The beam port comprises a conic delimiter of borated polyethylene and lead with a circular aperture of 15 cm in diameter spaced 15 cm from the cone base. At the exit aperture, a flat and radially well-delimited in-air neutron flux distribution is obtained [26]. Table 2 summarizes the in-air parameters tallied at the patient position and averaged over the beam aperture. Note that the proposed figures of merit follow the spirit of those introduced in the IAEA report, taking into account those neutrons therapeutically useful to treat shallow tumors (i.e., both thermal and epithermal neutron energies). The resulting in-phantom thermal neutron flux attains its maximum at 1.0 cm in depth and its value is $1.1 \times 10^9\ n_{th}\ cm^{-2}\ s^{-1}$ (Fig. 2B).

2.4.2. FiR 1 reference beam

This is the reference epithermal beam of this study. It belongs to the clinical facility built at the TRIGA research reactor FiR 1, where more than 250 patients have been treated with BNCT, among which more than 100 were affected by head and neck tumors [8,29]. This facility provided an epithermal neutron beam with low hydrogen-recoil and incident gamma doses [27]. Table 3 reports the IAEA in-air parameters for FiR 1. Fig. 2A and B depict the neutron flux spectrum tallied over the 14 cm exit aperture, and the corresponding in-phantom thermal neutron flux profile, respectively. The maximum is attained at 2.0 cm in depth and its value is $2.5 \times 10^9\ n_{th}\ cm^{-2}\ s^{-1}$.

2.4.3. RA-6 designed beam B3

The Argentine BNCT project is working towards opening a clinical BNCT trial for head and neck cancer patients at RA-6 reactor. Within this context, several studies are underway including computational assessment of the therapeutic potential of the present clinical beam B2 [26], and BNCT clinical-veterinary studies to treat dogs and cats with spontaneous head and neck tumors with no therapeutic option. Modifications of the BNCT external filter of the RA-6 reactor are currently being evaluated.

These modifications allow tuning the neutron beam in two configurations: a mixed thermal-epithermal beam such as the actual B2, and an epithermal beam -named B3- similar to those used in HN cancer BNCT (see Fig. 2). In-air parameters of the designed RA-6 B3 beam are listed in Table 3. In addition, evaluations based on the designed B3 beam show that the epithermal neutron flux attains a maximum of $2.3 \times 10^9\ n_{th}\ cm^{-2}\ s^{-1}$ at 1.8 cm depth in phantom.

2.4.4. RFQ designed beam

In the frame of the project to install a clinical BNCT facility in Italy based on the proton RFQ accelerator designed and manufactured by INFN, an epithermal neutron beam has been projected by simulating a suitable beam shaping assembly (BSA). Neutrons are produced by 5 MeV protons interacting with a Be target, and moderated to obtain a beam centered around 1 keV and with contaminations as low as possible (Fig. 2). The structure of BSA has been optimized through an extensive study comprising treatment planning in real cases of deep-seated tumor, peripheral doses delivered to healthy organs and radioprotection issues [30].

Table 3 reports the in-air parameters for the optimized beam configuration that comprises a circular aperture of 12 cm in diameter. From Fig. 2 it follows that the in-phantom thermal neutron flux peak is

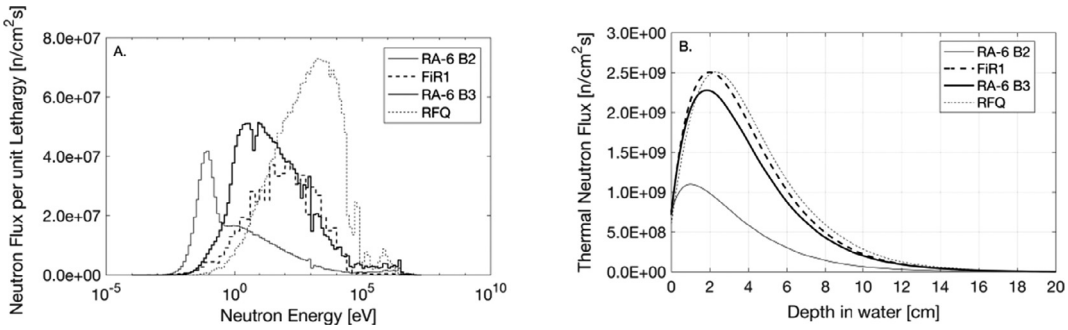

Fig. 2. Comparisons of (A) neutron flux-energy spectra averaged over the corresponding beam exit apertures and (B) thermal neutron flux profiles along the central axis of the standard water phantom, for the clinical beams RA-6 B2 and FiR 1 (operated by CNEA and VTT at the Argentine RA-6 and Finnish Reactors, respectively), and for the two realistic epithermal beam designs, RA-6 B3 and RFQ (Provenzano et al., 2014, Auterinen et al., 2001, Esposito et al., 2009).

Table 2
In-air parameters of the B2 clinical beam of the RA-6 reactor tallied and averaged over the circular aperture of 15 cm in diameter. Subscripts "*th*", "*epi*" and "*fast*" denote thermal (< 0.5 eV), epithermal (0.5 eV and 10 keV), and fast (> 10 keV) neutron flux (ϕ), respectively. $\dot{D}_\gamma/\phi_{th+epi}$ and $\dot{D}_{fast}/\phi_{th+epi}$ are the specific photon and fast dose, respectively. J/ϕ is the total current to total neutron flux ratio.

Figure of Merit	RA-6 clinical beam B2
ϕ_{th+epi} (n cm^{-2} s^{-1})	4.62×10^{8}
$\dot{D}_\gamma/\phi_{th+epi}$ (Gy cm^2 n^{-1})	1.74×10^{-12}
$\dot{D}_{fast}/\phi_{th+epi}$ (Gy cm^2 n^{-1})	5.71×10^{-13}
J/ϕ	0.75

2.5×10^{9} n_{th} cm^{-2} s^{-1} and occurs at 2.3 cm depth.

2.5. Standardized case study for head and neck tumors

A systematic study comprising a cylindrical phantom and a spherical tumor of variable size is presented as a practical application of the introduced radiobiological figures of merit for HN cancer BNCT. The purpose of this study carried out in a simplified clinical context is twofold: a) to propose a suitable procedure to assess the therapeutic potential and versatility of a beam, and b) to compare the performances of different BNCT beams.

For a given clinical scenario, the therapeutic potential is defined as the ability of the beam to control a tumor without unacceptable complications. The versatility, on other hand, is related with the variety of scenarios for which the therapeutic potential is acceptable.

2.5.1. Description of the standard geometry for HN cancer

Solid PMMA cylindrical phantoms have been extensively used in BNCT facilities for performing experimental dosimetry for head and neck cancer [31,32]. Then, a standard cylinder of 20 cm diameter and 24 cm high was selected for the systematic study. The tumor lesion representing the gross tumor volume (GTV) was modelled starting from a spherical volume positioned at 1 cm depth from the surface. The radius of the GTV was varied from 0.5 to 3.5 cm in a 0.5 cm-step. Thus, the maximum target depths ranged from 2 cm to 8 cm from this surface. A safety margin of 1 cm was added around the GTV to create a planning target volume (PTV) for each tumor lesion.

2.5.2. Dose calculations and evaluations

The MultiCell algorithm [33] was used to generate the 3-dimensional model of the standard geometry and for dose calculations with MCNP5 [28]. The elemental compositions and mass densities of air and PMMA materials were taken from ICRU 44 report [34]. Following the current clinical practice of HN cancer treatments with BNCT [21,8,35,36,22], a single and two lateral 90°-apart treatment fields were considered in the analysis. As depicted in Fig. 3, displacements of 0 and 7.5 cm between the geometry and irradiation field were evaluated.

Photon iso-effective doses to the GTV, PTV and to the mucosa tissue (for simplicity, defined as any point in the volume outside the GTV and PTV) were computed assuming a blood boron concentration value of 15 ppm and constant tumor-to-blood and mucosa-to-blood ratios of 3.5:1 and 2:1, respectively [8].

Calculations of the introduced radiobiological figures of merit were carried out for the treatment strategy employed in the Finnish clinical trial of HN cancer. In this protocol, patients received two BNCT applications separated by 3–5 weeks. Then, while the effect on the tumor was assumed additive for calculations of the *TCP*, complete repair of the mucosal membrane damage was assumed between BNCT applications to estimate the *NTCP*. The uncomplicated tumor control probability as a function of the total irradiation time was calculated for the four studied beams considering the mentioned clinical scenarios and irradiation conditions. From the results of the maximum *UTCP* for each tumor size, the therapeutic potential and versatility of each neutron source are discussed. Finally, comparisons of the performance of different BNCT beams on the basis of the maximum *UTCP* for each clinical scenario are presented.

Table 3
In-air parameters of the studied epithermal beams (FiR 1, RA-6 B3 and RFQ), tallied and averaged over the corresponding exit apertures. $\dot{D}_\gamma/\phi_{epi}$ and $\dot{D}_{fast}/\phi_{epi}$ are the specific photon and fast dose, respectively. ϕ_{th}/ϕ_{epi} is the ratio between the thermal flux and the epithermal flux. J/ϕ is the total current to total neutron flux ratio.

Figure of Merit	IAEA TecDoc-1223 Recommendation	FiR 1 Reactor Existing beam	RA-6 B3 Reactor Design	RFQ Accelerator Design
ϕ_{epi} (n cm^{-2} s^{-1})	$> 1.0 \times 10^{9}$	1.03×10^{9}	0.86×10^{9}	1.08×10^{9}
$\dot{D}_\gamma/\phi_{epi}$ (Gy cm^2 n^{-1})	$< 2.0 \times 10^{-13}$	0.5×10^{-13}	7.4×10^{-13}	4.17×10^{-13}
$\dot{D}_{fast}/\phi_{epi}$ (Gy cm^2 n^{-1})	$< 2.0 \times 10^{-13}$	1.4×10^{-13}	9.6×10^{-13}	9.5×10^{-13}
ϕ_{th}/ϕ_{epi}	< 0.05	0.06	0.10	0.01
J/ϕ	> 0.7	0.75	0.72	0.74

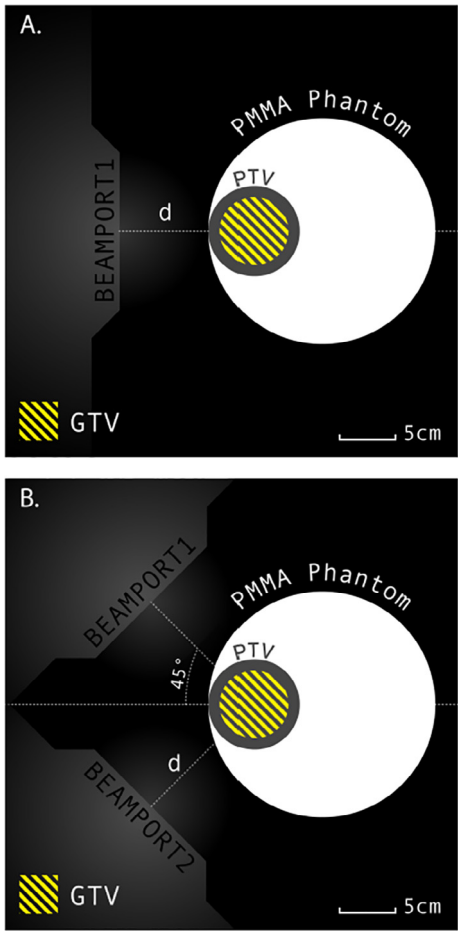

Fig. 3. Sagittal view of the PMMA cylindrical phantom showing, as an example, the spherical tumor of 3 cm radius positioned at 1 cm depth from the surface (GTV) and the safety margin of 1 cm around the lesion to create a PTV. A single (A) and two lateral 90°-apart treatment fields (B) positioned at a distance d = 0 cm or d = 7.5 cm from the geometry were considered in the analysis.

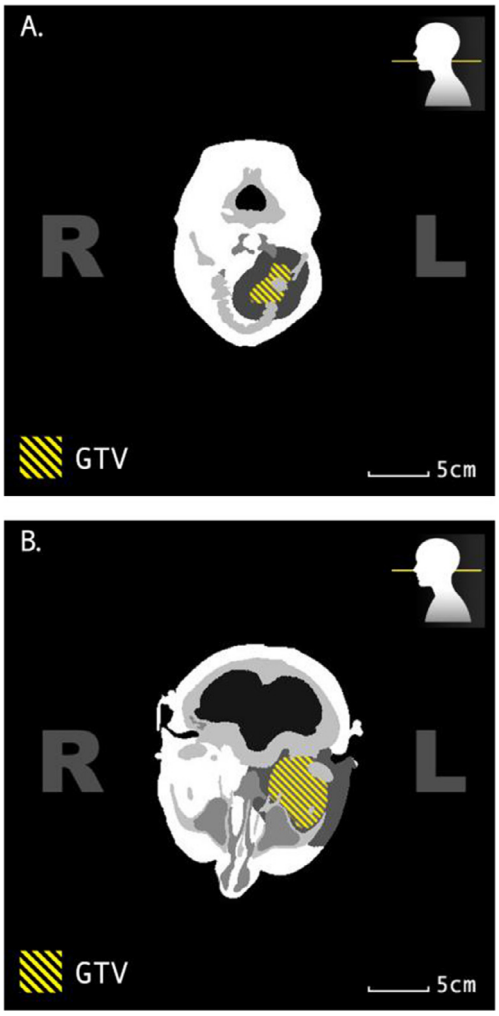

Fig. 4. Segmented CT scans showing the location of the tumor volume (GTV) of the head and neck cancer patients selected for dosimetry calculations with the RA-6 B2 clinical beam and RFQ designed beam.

2.6. Assessments of radiobiological FOM in humans

The following analysis is introduced to show the different applications of the proposed FOMs in a real clinical scenario of HN cancer patient treated with BNCT.

Within this context, two inoperable, locally recurred head and neck cancer patients treated with BPA-mediated BNCT in a single-centre Phase I/II study carried out in Finland were selected to perform computational simulations and beam performance evaluations. Details on the clinical protocol and patient results can be found in Kankaanranta et al. [8].

A small and a large squamous cell carcinoma tumor covering superficial and deep-seated maximum target depth were chosen for the analysis (Fig. 4). Table 4 shows the general characteristics of the selected HN patients and the tumor response after BNCT.

For this study, FiR 1 is considered the reference beam. The analysis was focused: a) to analyze the therapeutic potential of the FiR 1 and to discuss the delivered treatment on the basis of the maximum *UTCP*, and b) to compare the performances of the existing and designed neutron beams RA-6 B2 and RFQ (especially tuned to treat, respectively, shallow and deep-seated tumor targets), with respect to the performance of FiR 1.

As before, the MultiCell algorithm was used for the generation of the 3-dimensional model of the patients and for dose planning using the neutron beams [33]. This model accurately resembles the 3D patient model generated with the treatment planning system used in Finland

Table 4
Selected patients with inoperable, locally recurred head and neck cancer treated with BPA-mediated BNCT in Finland (Kankaanranta et al., 2012).

Patient	Tumor (GTV) (cm^3)	Maximum target depth (cm)	Tumor Response	Mucositis ≥ G3
HN01	14	~4.0	CR	NO
HN02	116	~7.5	SD	NO

CR: complete response; SD: stable disease.

SERA [37], allowing the dosimetry to be comparable between calculation systems.

The Finnish protocol for the treatment of HN cancer patients together with the parameters of each delivered treatment were considered for the computational simulations. Thus, calculations using the RA-6 B2 and RFQ beams were carried out selecting the beam directions and number of fields used in the delivered treatments. Photon iso-effective doses to the GTV, PTV and to the mucosa tissue were computed as for the systematic study but using the whole blood average boron concentration measured during patient irradiations.

The models of *TCP* for non-uniform doses and *NTCP* were used to calculate the *UTCP* as a function of the irradiation time for each analyzed beam. From the *UTCP* curve obtained for the reference beam, the delivered treatment to each patient was compared to the optimum on the basis of the maximum *UTCP*. The comparison of the performances

of the neutron beams RA-6 B2 and RFQ with respect to the performance of FiR 1 was carried out analyzing both the maximum values of the *UTCP* and the values of the *TCP* for a given *NTCP*.

3. Results and discussions

3.1. Derivation of the tumor control probability model for HN cancer when the dose distribution is inhomogeneous

Let the tumor control probability for the combination of the boron, thermal neutron, fast neutron and gamma uniform absorbed dose components of the mixed field BNCT radiation $D_1, \cdots, D_4$ be given by

$$TCP(v, D_1, \cdots, D_4) = e^{-(c_1 v^{c_2} S(D_1, \cdots, D_4))} \quad (4)$$

In this model, v represents the tumor volume (in cm^3) with $c_1$and c_2 parameters that modulate its effect on local control probability, and $S(D_1, \cdots, D_4)$ the survival expression for the mixed field radiation. Now, let $D_1(\boldsymbol{x}), \cdots, D_4(\boldsymbol{x})$ denote the spatial absorbed dose for each component at the point $\boldsymbol{x}$. Applying the equivalent subvolume model to expression (4), it follows that the *TCP* for the tumor T is

$$TCP_T = e^{-c_1 v^{c_2}} \left(\int_T S(D_1(\boldsymbol{x}), \cdots, D_4(\boldsymbol{x}))^{1/c_2} \frac{d\boldsymbol{x}}{v} \right)^{c_2} \quad (5)$$

Allowing the different components to act synergistically

$$-\ln(S(D_1(\boldsymbol{x}), \cdots, D_4(\boldsymbol{x}))) = \sum_{i=1}^{4} \alpha_i D_i(\boldsymbol{x}) + \sum_{i=1}^{4} \sum_{j=1}^{4} G_{ij}(\theta) \sqrt{\beta_i \beta_j} D_i(\boldsymbol{x}) D_j(\boldsymbol{x}), \quad (6)$$

where α_i and β_i are the coefficients of the single fraction linear quadratic model for radiation i ($i = 1, \cdots, 4$), and $G_{ij}(\theta)$ is the time factor for a simultaneous mixed irradiation that accounts for the repair of pairs of sublesions produced by radiations i and j during the irradiation timeθ [5]. For the calculation of $G_{ij}(\theta)$, a bi-exponential repair kinetics with fast and slow characteristic repair times independent of LET of $24/ln2$ min and $14/ln2$ h, respectively, was assumed. In addition, the proportions of the sublesions repaired by the two kinetics were taken as 0.57 and 0.43 for the low LET radiation (i.e., for $i = 4$), and 0.2 and 0.8, for the high LET radiations (i.e., for $i = 1, 2, 3$), following the results reported by Schmid et al. [38] for a squamous cell carcinoma cell line.

Substituting expression (6) in (5), the tumor control probability for inhomogeneous dose distributions in BNCT is obtained. Note that the TCP_T model for photon radiation is also obtained taking $i = j = 1$ in Eq. (6). Table 5 summarizes the radiobiological parameters of the *TCP* model for the reference radiation (photons) and for BNCT used for calculations in this work.

The impact of considering tumor dose inhomogeneity for *TCP* calculations is presented in Fig. 5. The dose distributions for the GTVs modelled in the cylindrical phantom were used to evaluate Eq. (5). The treatment selected comprised irradiations of 30 min with FiR 1 using the two lateral fields positioned 7.5 cm apart from the phantom. Two

Table 5
Radiobiological parameters of the *TCP* model (± 1SD) for the reference radiation and for BNCT based on the in vivo oral cancer model in the hamster cheek pouch (González et al., 2017).

	TCP $c_1 = 22 \pm 19$, $c_2 = 0.33 \pm 0.09$	
	Alpha (Gy^{-1})	Beta (Gy^{-2})
^{60}Co or 6MV LINAC		
Reference radiation	0.029 ± 0.008	0.0029 ± 0.0008
FCCT (RA-3 reactor)		
Beam gamma photons	0.029 ± 0.008	0.0029 ± 0.0008
Neutrons	0.37 ± 0.03	(8.8 ± 2.2) × 10^{-9}
Boron (L-BPA-F)	0.34 ± 0.03	(8.3 ± 3.1) × 10^{-9}

FCCT & L-BPA-F as defined in Table 1.

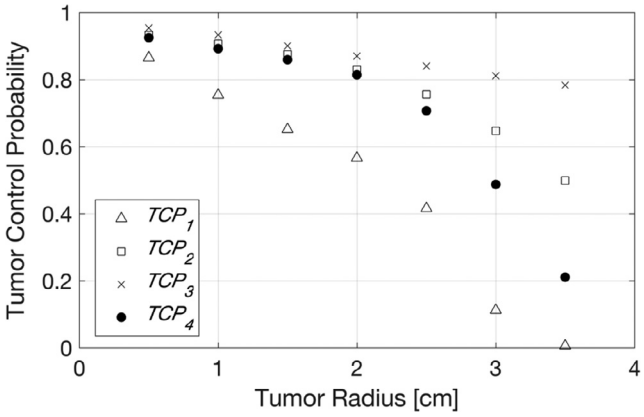

Fig. 5. Tumor control probability for the different spherical tumors modelled in the cylindrical HN phantom. TCP_1, TCP_2 and TCP_3 were calculated assuming uniform dose distributions equal to the minimum, mean and maximum tumor dose, respectively. TCP_4 was computed using the whole tumor dose distribution.

levels of approximations were taken into account for the calculations of *TCPs*. In TCP_1, TCP_2 and TCP_3 the tumor dose inhomogeneity was not taken into account and thus, the dose distribution through the GTV was assumed to be uniform and equal to the minimum, mean and maximum tumor dose, respectively. For TCP_4, the whole tumor dose distribution was considered.

Fig. 5 reveals that the dose inhomogeneity affects the *TCP* particularly for the larger tumors for which, since the dose distribution can vary significantly with depth, this inhomogeneity is likely to be higher than for the smaller lesions. The results show that the *TCP* obtained from the mean tumor dose overestimates the actual value of the *TCP* (i.e., $TCP_2 \geq TCP_4$). Also, that Eq. (5) evaluated in the minimum tumor dose underestimates the actual value of the *TCP* (i.e., $TCP_1 \leq TCP_4$). The fact that TCP_4 are always between TCP_1 and TCP_2 demonstrate that the actual *TCP* is more influenced by low doses. Since average doses on their own might not have a clear clinical relevance and the *TCP* based on the minimum doses might considerably underestimate the actual values of the *TCP*, it follows that the performance of a beam would be inappropriately assessed in the light of these values. Thus, a model that takes into account the particularities of the tumor dose distribution, such as the one introduced in this work, would guarantee an adequate evaluation of the therapeutic potential of the neutron beam.

3.2. Results for the standardized case study for head and neck tumors

Fig. 6 shows the results of the maximum *UTCP* as a function of the tumor size (or equivalently, the maximum target depth) for the four studied neutron beams, as part of the systematic study comprising the simplified HN cancer model and different irradiation conditions.

The therapeutic potential of a beam for a given tumor and treatment condition is associated with the absolute value of the maximum *UTCP*: the greater the maximum *UTCP*, the higher the potential of the beam to deliver a successful treatment (i.e., to control the lesion without unacceptable complications). Fig. 6 presents the fraction of HN tumors that would be controlled without observing mucositis ≥ G3 as a function of the tumor size, for each studied beam and irradiation condition. Hence, if a threshold of acceptability is established according to the medical criteria, for example, equal to 0.4, it follows that both FiR 1 and RFQ would be well suited to treat lesions of up to 2 cm radius or 5-cm maximum target depth with a single direct beam incidence (Fig. 6A and B). When the treatment using the two lateral fields is analyzed under the same medical criteria, it comes out that RA-6 B3 would be also well suited to treat these tumors (Fig. 6C and D). The RA-6 B2 mixed beam would deliver, as expected, successful treatments for

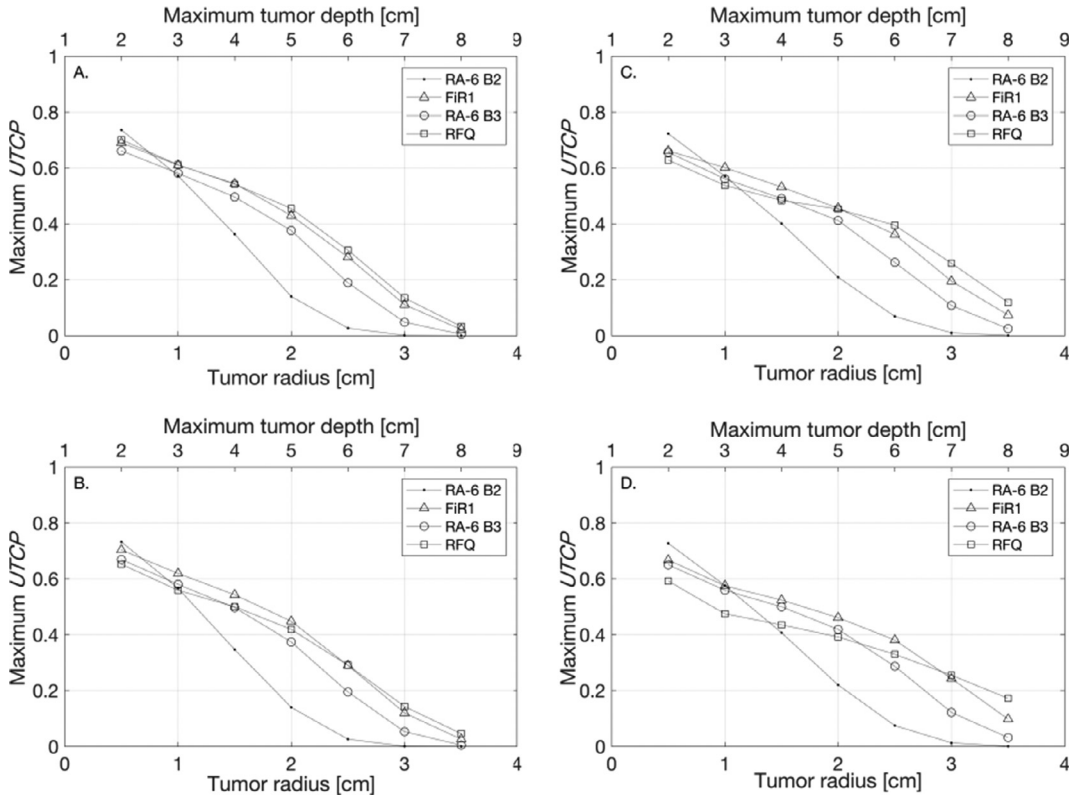

Fig. 6. Maximum UTCP as a function of the tumor size (or equivalently, the maximum target depth) for the four studied neutron beams, as part of the systematic study comprising the simplified HN cancer model. Top panels correspond to the irradiations using a single (A) and the two lateral treatment fields (C) in the absence of an air-gap between the fields and the geometry. Bottom panels (B & D) depict the same but considering the air-gap of 7.5 cm.

shallow lesions with maximum target depths lower than 4 cm.

Additional information that can be drawn from the maximum *UTCP* curves is the versatility of a beam. For a given irradiation condition and a threshold of acceptability, the greater the maximum target depth treatable (i.e., the maximum target depth for which the maximum *TCP* is equal or greater than the threshold), the greater the versatility of the beam to control different sized tumors without complications. From the results depicted in Fig. 6D and assuming again a threshold of 0.4, it follows that the versatility of both FiR 1 and RA-6 B3 increases when the irradiation condition using two lateral fields is considered. Then, the treatable maximum target depth increases from 5 cm to 6 cm for FiR 1, and from 4 cm to 5 cm for RA-6 B3. The slope of the maximum *UTCP* curve can be interpreted as the capability of the beam to treat different clinical scenarios with equal effectiveness. Then, the smaller the value of the slope the greater the number of treatable tumors.

The comparison of the performance of the different beams for each clinical scenario on the basis of the maximum *UTCP* is now presented. Fig. 6 shows that, regardless the irradiation condition, RA-6 B2 presents the highest values of the maximum *UTCP* and thus, the highest therapeutic potential for lesions of about 2.5-cm maximum target depth. This mixed beam has a very different spectrum compared to the three studied epithermal beams. This analysis demonstrates that even for completely different beams, it is possible to assess and compare their performances fairly and adequately by assessing the radiobiological figure of merit *UTCP*.

When analyzing the irradiation condition corresponding to the absence of an air-gap between the irradiation fields and the geometry, it turns out that both FiR 1 and RFQ have a comparable therapeutic potential and versatility. However, when the portals are separated from the model, the differences in the performance of the beams become evident. Note that while the values of J/ϕ do not explain these results (because they are almost the same for both beams; see Table 3), the maximum value of *UTCP* proves to be a sensitive figure of merit that highlights this finding. Regarding RA-6 B3, it can be concluded that this epithermal beam design has a comparable performance to those of FiR 1 and RFQ for maximum target depths of about 4–5 cm. On the other hand, the fact that its therapeutic potential falls off more rapidly compared the other epithermal beams, diminishes the ability of RA-6 B3 beam to control larger and deeper tumors without increasing the probability of developing undesirable radiotoxic effects.

3.3. FOMs assessments in humans

Fig. 7A and B shows the *UTCP* as a function of the total treatment time, for the two head and neck cancer patients treated within the clinical trial carried out in Finland using FiR 1. The corresponding *TCP* and *NTCP* curves for each patient are also depicted. From these results, it follows that the total irradiation time of the delivered treatments with FiR 1 is very close to the total time for which the probability of controlling the tumor without complication is optimal. Treatment decisions were carried out on the basis of the previous knowledge and great experience accumulated by the Finnish team in the clinical practice of BNCT. The closeness of the optimal treatment to the medical criterion establishes an important degree of confidence for the use of the *UTCP* in the clinic.

As reported in Table 4, maximum tumor depths of the patients HN01 and HN02 were about 4 cm and 7.5 cm, respectively. As the maximum *UTCP* for these real clinical scenarios is in line with the results of the simplified HN cancer model for the irradiation condition that closest resembles the treatment of the patients (i.e., for two lateral fields separated 7.5 cm), the systematic study is indeed a suitable procedure to evaluate the therapeutic potential and versatility of a BNCT beam. Note that in the case of the patients, the actual GTV and the dose-limiting point in mucosal membrane selected by the medical doctors were used for *UTCP* calculations.

Fig. 7C and D shows the *UTCP* curves that result when the

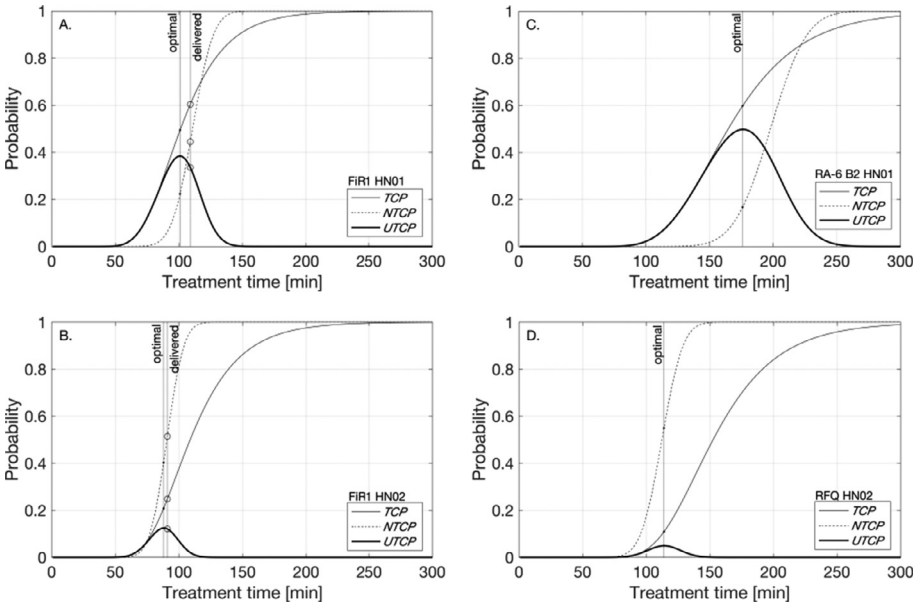

Fig. 7. Uncomplicated tumor control probability (UTCP) as a function of the total treatment time for the two HN cancer clinical cases selected for the study. TCP and NTCP curves are also shown. (A & B) Results using FiR 1 clinical beam. (C & D) Results obtained for the simulations of the treatments using RA-6 B2 and RFQ beams, respectively. Vertical lines indicate total irradiation times for the delivered treatment with FiR 1 and for which the probability of controlling the tumor without complication is optimal.

treatments of patients HN01 and HN02 are simulated using the RA-6 B2 and RFQ beams, respectively. The comparison of the maximum values of the *UTCP* with respect to those obtained with FiR 1 reveals that the therapeutic potential of RA-6 B2 and RFQ is, for each patient, comparable to that obtained with the Finnish clinical beam. The fact that these results are again in line with those obtained in the systematic study for tumors of comparable size and maximum depth (Fig. 6D) reinforces the previous assertion about the applicability of the proposed procedure to adequately evaluate and compare BNCT clinical beams.

Oral mucositis is a common dose-limiting toxicity of many radiation regimens, and several publications consider a clinically significant endpoint mucositis grade 3 or higher [39,40,24]. Within the Finnish protocol for the treatment of recurrent HN cancer patients, the maximum absorbed dose to the mucosal membrane was limited to 6 Gy per BNCT application. The analyzed beams have different neutron spectra and photon contaminations. Thus, the relative contribution of each dose component in BNCT to the maximum absorbed dose in mucosa is expected to be different for the different beams. Because the severity of biological damage depends on the radiation type (the high LET products are more biologically damaging than low LET radiation), equal values of absorbed dose do not lead to the same level of biological damage or effect. Therefore, limiting the RA-6 B2 and RFQ irradiation times to equal the maximum absorbed doses delivered with FiR 1 would be incorrect. A different approach that would allow a more reliable assessment of the feasibility of HN cancer treatments with the RA-6 B2 and RFQ beams is limiting irradiation times to equal the *NTCP* value of the actual treatments with FIR 1. For example, Fig. 7A shows that the delivered treatment to the patient HN01 with FiR 1 had a probability of tumor control of 0.60 and a probability of mucositis ≥ G3 after first BNCT application of 0.46 (i.e., *UTCP* = 0.33). If the irradiation time with RA-6 B2 is then limited so that the *NTCP* reaches a value of 0.46 (Fig. 7C), the resulting probability of tumor control is 0.67 (i.e., *UTCP* = 0.36). The irradiation time of each application of BNCT with the clinical beam RA-6 B2 is, as expected, higher than that of FiR 1, but it remains acceptable within the range of melanoma irradiations with BNCT in RA-6. Therefore, the fact that the *TCP* obtained with the RA-6 B2 beam is the same or even slightly better than that obtained with FiR 1 and that the tumor showed CR (Table 4), would open a window of opportunity for the use of this beam in the treatment of head and neck superficial tumors of moderate size in humans. Moreover, these results evidence that the RA-6 B2 clinical beam, with specific gamma and fast neutron doses higher than the IAEA recommendations for epithermal beams, can provide a potentially therapeutic treatment comparable (at least) to that delivered in Finland for the case of tumors with shallow maximum depth.

The low maximum *UTCP* values found for the large and deep challenging lesion of patient HN02 with beams FiR 1 and RFQ indicate that, unless the original irradiation and/or treatment conditions are altered, it would not be possible to obtain encouraging values of *TCP* avoiding the development of mucositis of clinical relevance (Fig. 7C and D). Note that the calculated *TCP* for the treatment delivered with FiR 1 is in line with the observed tumor response assessed as stable disease.

For these complex clinical scenarios, other treatment strategies could be explored, for example, by adding additional irradiation portals to the original treatment planning, or, by exploring other boron compounds different to BPA or even combining compounds to achieve a higher relative targeting between tumor and the dose-limiting normal tissue than that obtained with BPA. To have a figure of merit such as the *UTCP* would allow forecasting, on a robust basis, if any of the proposed alternatives shows a net benefit compared to the original treatment.

Finally, the different applications of the radiobiological figures of merit presented in this work can easily be extended to the analysis of the performance of a beam for treating other targets, by constructing an appropriate *UTCP*. Models of *TCP* and *NTCP* for BNCT considering other tissues of interest have been developed and published in the last years. In particular, *TCP* models for cutaneous melanomas, brain tumors, and osteosarcomas based on in-vitro radiobiological data are available in González et al. [4] and Bortolussi et al. [41], and are ready to be used in combination with any or some *NTCP* models that describe the complication in a single or multiple nearby healthy organs or tissues. For example, the *UTCP* for cutaneous melanoma treatments with BNCT can be constructed using the *TCP* model introduced in González et al. [4] and the *NTCP* model for normal skin based on human data presented by González et al. [42]. In addition, the authors are working to complete the *NTCP* models for other tissues that limit the dose (such as normal brain and lung). Proposed *UTCP* model can be extended not only for different clinical scenarios related with different pathologies but also to study the benefit of applying different boron compounds and administration protocols. Since boron concentration ratio between cancer cells and normal tissues might be a function of time [15,43,44], the proposed model is capable to consider the variation of the boron ratio along the treatment.

The codes of the probability models used in this work can be found

in a public web repository [45].

4. Conclusions

Boron Neutron Capture Therapy is a treatment modality that produces low and high LET radiations that contribute to the total dose. Since each type of radiation interacts with tissues producing a particular level of biological damage, the assessment of the performance of a BNCT beam and its comparison with other facilities requires the evaluation of appropriate radiobiological figures of merit in addition to the primary physical quantities of the beam.

This work presents the development and innovative use of probability models to evaluate and compare the therapeutic potential and versatility of BNCT beams.

The *TCP* model for non-uniform doses introduced in this work highlights the importance of considering the whole dose distribution of the target to estimate the expected success with a BNCT treatment. Depending on the characteristics of the beam, such as penetration and collimation, and the irradiation strategy, the differences between maximum and minimum tumor dose values can be minimized. However, large and deep lesions are likely to show significant inhomogeneity. Having an appropriate model able to deal with such inhomogeneity would guarantee an adequate estimation of the tumor control.

The concept of uncomplicated tumor control probability was introduced and applied in BNCT for the first time proposing a suitable expression for HN cancer. It was shown how from the maximum values of the *UTCP* it is possible to assess the therapeutic potential and versatility of a beam, characteristics that collectively describe the clinical performance of a particle source. The maximum *UTCP* also showed to be a sensitive figure of merit allowing pointing out particularities of the beam performances that the standard figures of merit do not. This extends the usefulness of the FOMs introduced, for example, for ranking treatment plans or for evaluating new boron compounds.

The systematic study presented based on a simplified model of HN cancer showed to be a practical and adequate procedure to evaluate and compare the performances of different BNCT beams. The current developments of *TCP* and *NTCP* models for other treatment targets would guarantee that the studies presented for the case of HN can be extended to other cases of interest in BNCT.

The FOMs evaluated for the real cases of patients showed to be useful tools both for retrospective analysis of the BNCT treatments carried out with existing facilities, and for prospective feasibility studies using realistic beam designs. Considering that currently, there are open protocols of HN cancer treatments with BNCT in Japan and Taiwan and that a new protocol based on accelerator-BNCT is about to start in Finland, the presented developments along with the proposed applications would be also a practical and useful aid to guide treatment decisions.

Acknowledgements

The authors gratefully acknowledge the collaboration of Leena Kankaanranta, M.D., and Professor Heikki Joensuu, M.D., Ph.D. of Helsinki University Central Hospital, who kindly provided valuable clinical information for the development of this work. Iiro Auterinen, M.Sc., is also gratefully acknowledge for providing the computational description of Fir 1 neutron source. This work was partially funded by the Agencia Nacional de Promoción Científica y Tecnológica of Argentina through a PICT grant N° 2013-1777 and by the Consejo Nacional de Investigaciones Científicas y Técnicas of Argentina through a PIP grant 2014-2016 GI, N° 112 201301 00458 CO.

References

[1] Locher G. Biological effects and therapeutical possibilities of neutrons. Am J Roent Radium Ther 1936;36:1–13.
[2] TECDOC Series 1223. Current status of neutron capture therapy. International Atomic Energy Agency (IAEA); 2001.
[3] Wheeler FJ, Nigg DW, Capala J, Watkins PRD, Vroegindeweij C, Auterinen I, et al. Boron neutron capture therapy (BNCT): implications of neutron beam and boron compound characteristics. Med Phys 1999;26:1237–44. https://doi.org/10.1118/1.598618.
[4] González SJ, Cruz GAS. The photon-isoeffective dose in boron neutron capture therapy. Radiat Res 2012;178:609–21. https://doi.org/10.1667/RR2944.1.
[5] González SJ, Pozzi ECC, Hughes AM, Provenzano L, Koivunoro H, Carando DG, et al. Photon iso-effective dose for cancer treatment with mixed field radiation based on dose–response assessment from human and an animal model: clinical application to boron neutron capture therapy for head and neck cancer. Phys Med Biol 2017;62:7938–58. https://doi.org/10.1088/1361-6560/aa8986.
[6] Esposito J, Colautti P, Fabritsiev S, Gervash A, Giniyatulin R, Lomasov VN, et al. Be target development for the accelerator-based SPES-BNCT facility at INFN Legnaro. Appl Radiat Isot 2009;67:S270–3. https://doi.org/10.1016/j.apradiso.2009.03.085.
[7] Blaumann HR, González SJ, Longhino J, Cruz GAS, Larrieu OAC, Bonomi MR, et al. Boron neutron capture therapy of skin melanomas at the RA-6 reactor: a procedural approach to beam set up and performance evaluation for upcoming clinical trials. Med Phys 2004;31:70–80. https://doi.org/10.1118/1.1631915.
[8] Kankaanranta L, Seppälä T, Koivunoro H, Saarilahti K, Atula T, Collan J, et al. Boron neutron capture therapy in the treatment of locally recurred head-and-neck cancer: final analysis of a phase I/II trial. Int J Radiat Oncol Biol Phys 2012;82:e67–75. https://doi.org/10.1016/j.ijrobp.2010.09.057.
[9] Coderre JA, Morris GM. The radiation biology of boron neutron capture therapy. Rad Res 1999;151:1–18. https://doi.org/10.2307/3579742.
[10] González SJ, Bonomi MR, Santa Cruz GA, Blaumann HR, Larrieu OAC, Menéndez P, et al. First BNCT treatment of a skin melanoma in Argentina: dosimetric analysis and clinical outcome. Appl Radiat Isot 2004;61:1101–5. https://doi.org/10.1016/j.apradiso.2004.05.060.
[11] Menéndez PR, Roth BMC, Pereira MD, Casal MR, González SJ, Feld DB, et al. BNCT for skin melanoma in extremities: Updated Argentine clinical results. Appl Radiat Isot 2009;67:S50–3. https://doi.org/10.1016/j.apradiso.2009.03.020.
[12] Sato T, Masunaga S, Kumada H, Hamada N. Microdosimetric modeling of biological effectiveness for boron neutron capture therapy considering intra- and intercellular heterogeneity in 10B distribution. Sci Rep 2018;8:988. https://doi.org/10.1038/s41598-017-18871-0.
[13] Ono K, Tanaka H, Tamari Y, Watanabe T, Suzuki M, Masunaga S. Proposal for determining absolute biological effectiveness of boron neutron capture therapy—the effect of 10B(n, α)7Li dose can be predicted from the nucleocytoplasmic ratio or the cell size. J Radiat Res 2018;60:29–36. https://doi.org/10.1093/jrr/rry080.
[14] Laramore G, Wheeler F, Wessol D, Stelzer K, Griffin T, Larsson B, et al. A tumor control curve for malignant gliomas derived from fast neutron radiotherapy data: implications for treatment delivery and compound selection. New York: Elsevier Science; 1997. p. 580–7.
[15] Farías RO, Bortolussi S, Menéndez PR, González SJ. Exploring boron neutron capture therapy for non-small cell lung cancer. Phys Med 2014;30:888–97. https://doi.org/10.1016/j.ejmp.2014.07.342.
[16] Tommasino F, Nahum A, Cella L. Increasing the power of tumour control and normal tissue complication probability modelling in radiotherapy: recent trends and current issues. Transl Cancer Res 2017;6:S807–21. doi: 10.21037/14116.
[17] Kreimann EL, Itoiz ME, Dagrosa A, Garavaglia R, Farías S, Batistoni D, et al. The hamster cheek pouch as a model of oral cancer for boron neutron capture therapy studies: selective delivery of boron by boronophenylalanine. Cancer Res 2001;61:8775–81.
[18] Vairaktaris E, Spyridonidou S, Papakosta V, Vylliotis A, Lazaris A, Perrea D, et al. The hamster model of sequential oral oncogenesis. Oral Oncol 2008;44:315–24. https://doi.org/10.1016/j.oraloncology.2007.08.015.
[19] Chen Y-K, Lin L-M. DMBA-induced hamster buccal pouch carcinoma and VX2-induced rabbit cancer as a model for human oral carcinogenesis. Expert Rev Anticancer Ther 2010;10:1485–96. https://doi.org/10.1586/era.10.108.
[20] Supsavhad W, Dirksen WP, Martin CK, Rosol TJ. Animal models of head and neck squamous cell carcinoma. Vet J 2016;210:7–16. https://doi.org/10.1016/j.tvjl.2015.11.006.
[21] Kato I, Fujita Y, Maruhashi A, Kumada H, Ohmae M, Kirihata M, et al. Effectiveness of boron neutron capture therapy for recurrent head and neck malignancies. Appl Radiat Isot 2009;67:S37–42. https://doi.org/10.1016/j.apradiso.2009.03.103.
[22] Wang L-W, Chen Y-W, Ho C-Y, Hsueh Liu Y-W, Chou F-I, Liu Y-H, et al. Fractionated boron neutron capture therapy in locally recurrent head and neck cancer: a prospective phase I/II trial. Int J Radiat Oncol Biol Phys 2016;95:396–403. https://doi.org/10.1016/j.ijrobp.2016.02.028.
[23] González SJ, Carando DG. A general tumour control probability model for non-uniform dose distributions. Math Med Biol 2008;25:171–84. https://doi.org/10.1093/imammb/dqn012.
[24] Strigari L, Pedicini P, D'Andrea M, Pinnarò P, Marucci L, Giordano C, et al. A new model for predicting acute mucosal toxicity in head-and-neck cancer patients undergoing radiotherapy with altered schedules. Int J Radiat Oncol Biol Phys 2012;83:e697–702. https://doi.org/10.1016/j.ijrobp.2012.02.004.
[25] Stüben G, van der Kogel AJ, van der Schueren E. Biological equivalance of low dose rate to multifractionated high dose rate irradiations: investigations in mouse lip mucosa. Radiother Oncol 1997;42:189–96. https://doi.org/10.1016/S0167-8140(96)01869-5.
[26] Provenzano L, Farías RO, Longhino JM, Boggio EF, Herrera MS, Moijsecsiuck N, et al. A prospective study to assess the performance of the improved boron neutron

capture therapy facility in Argentina. Appl Radiat Isot 2014;88:171–6. https://doi.org/10.1016/j.apradiso.2013.11.041.
[27] Auterinen I, Hiismäki P, Kotiluoto P, Rosenberg RJ, Salmenhaara S, Seppälä T. Metamorphosis of a 35 year-old TRIGA reactor into a modern BNCT facility. In: Hawthorne MF, Shelly K, Wiersema RJ, editors. Frontiers in neutron capture therapy: Volume 1 Boston, MA: Springer US; 2001. p. 267–75. https://doi.org/10.1007/978-1-4615-1285-1_36.
[28] X-5 Monte Carlo Team. MCNP – version 5, Vol. I: overview and theory. LA-UR-03-1987. Los Alamos National Laboratory; 2003.
[29] Koivunoro H, Kankaanranta L, Seppälä T, Haapaniemi A, Mäkitie A, Joensuu H. Boron neutron capture therapy for locally recurrent head and neck squamous cell carcinoma: an analysis of dose response and survival. Radiother Oncol 2019;137:153–8. https://doi.org/10.1016/j.radonc.2019.04.033.
[30] Postuma I. Clinical application of accelerator-based boron neutron capture therapy: optimization of procedures, tailoring of a neutron beam and evaluation of its dosimetric performance [PhD. thesis]. Università degli studi di Pavia; 2016.
[31] Raaijmakers CPJ, Nottelman EL, Mijnheer BJ, Nottelman EL. Phantom materials for boron neutron capture therapy. Phys Med Biol 2000;45:2353–61. https://doi.org/10.1088/0031-9155/45/8/320.
[32] Lee J-C, Chen Y-W, Chuang K-S, Hsu F-Y, Chou F-I, Hsu S-M, et al. The dosimetric impact of shifts in patient positioning during boron neutron capture therapy for brain tumors. Biomed Res Int 2018. https://doi.org/10.1155/2018/5826174.
[33] Farias R, González S. MultiCell model as an optimized strategy for BNCT treatment planning. Proceedings of the 15th international congress on neutron capture therapy. 2012. p. 149–50. Tsukuba, Japan.
[34] White DR, Booz J, Griffith RV, Spokas JJ, Wilson IJ. Report 44. J ICRU 1989. https://doi.org/10.1093/jicru/os23.1.Report44.
[35] Suzuki M, Kato I, Aihara T, Hiratsuka J, Yoshimura K, Niimi M, et al. Boron neutron capture therapy outcomes for advanced or recurrent head and neck cancer. J Radiat Res 2014;55:146–53. https://doi.org/10.1093/jrr/rrt098.
[36] Aihara T, Morita N, Kamitani N, Kumada H, Ono K, Hiratsuka J, et al. BNCT for advanced or recurrent head and neck cancer. Appl Radiat Isot 2014;88:12–5. https://doi.org/10.1016/j.apradiso.2014.04.007.
[37] Nigg DW. Computational dosimetry and treatment planning considerations for neutron capture therapy. J Neuro-Oncol 2003;62:75–86. https://doi.org/10.1023/A:1023241022546.
[38] Schmid TE, Dollinger G, Beisker W, Hable V, Greubel C, Auer S, et al. Differences in the kinetics of γ-H2AX fluorescence decay after exposure to low and high LET radiation. Int J Radiat Biol 2010;86:682–91. https://doi.org/10.3109/09553001003734543.
[39] Wu X, Chen P, Sonis ST, Lingen MW, Berger A, Toback FG. A novel peptide to treat oral mucositis blocks endothelial and epithelial cell apoptosis. Int J Radiat Oncol Biol Phys 2012;83:e409–15. https://doi.org/10.1016/j.ijrobp.2012.01.006.
[40] Alvarez E, Fey EG, Valax P, Yim Z, Peterson JD, Mesri M, et al. Preclinical characterization of CG53135 (FGF-20) in radiation and concomitant chemotherapy/radiation-induced oral mucositis. Clin Cancer Res 2003;9:3454–61.
[41] Bortolussi S, Postuma I, Protti N, Provenzano L, Ferrari C, Cansolino L, et al. Understanding the potentiality of accelerator based-boron neutron capture therapy for osteosarcoma: dosimetry assessment based on the reported clinical experience. Radiat Oncol 2017;12:130. https://doi.org/10.1186/s13014-017-0860-6.
[42] González SJ, Casal M, Pereira MD, Santa Cruz GA, Carando DG, Blaumann H, et al. Tumor control and normal tissue complications in BNCT treatment of nodular melanoma: a search for predictive quantities. Appl Radiat Isot 2009;67:S153–6. https://doi.org/10.1016/j.apradiso.2009.03.038.
[43] Kiger WSI, Palmer MR, Zamenhof RG, Busse PM. Boron uptake by erythrocytes following boronophenylalanine-fructose infusion in humans. IAEA Report KURRI-KR-54. 2000. Japan.
[44] Imahori Y, Ueda S, Ohmori Y, Kusuki T, Ono K, Fujii R, et al. Fluorine-18-labeled fluoroboronophenylalanine PET in patients with glioma. J Nucl Med 1998;39:325–33.
[45] Provenzano L, González SJ. BNCT dosimetry tools developed by computational dosimetry and treatment planning department of argentinean BNCT group. 2019https://github.com/lucasprovenzano/BnctAR.